



HAL
open science

Simulation-based optimization of the design and settings of ultrasonic phased-array transducers with an evolutionary algorithm

Benoît Puel, Dominique Lesselier, Sylvain Chatillon, Pierre Calmon

► To cite this version:

Benoît Puel, Dominique Lesselier, Sylvain Chatillon, Pierre Calmon. Simulation-based optimization of the design and settings of ultrasonic phased-array transducers with an evolutionary algorithm. AIP Conference Proceedings, 2011, REVIEW OF PROGRESS IN QUANTITATIVE NONDESTRUCTIVE EVALUATION, 1335 (1), pp.906-913. 10.1063/1.3591943 . hal-00546793

HAL Id: hal-00546793

<https://hal.science/hal-00546793v1>

Submitted on 24 Jan 2024

HAL is a multi-disciplinary open access archive for the deposit and dissemination of scientific research documents, whether they are published or not. The documents may come from teaching and research institutions in France or abroad, or from public or private research centers.

L'archive ouverte pluridisciplinaire **HAL**, est destinée au dépôt et à la diffusion de documents scientifiques de niveau recherche, publiés ou non, émanant des établissements d'enseignement et de recherche français ou étrangers, des laboratoires publics ou privés.

SIMULATION-BASED OPTIMIZATION OF THE DESIGN AND SETTINGS OF ULTRASONIC PHASED-ARRAY TRANSDUCERS WITH AN EVOLUTIONARY ALGORITHM

B. Puel¹, D. Lesselier², S. Chatillon¹, and P. Calmon¹

¹CEA, LIST, DISC, F-91191, Gif-sur-Yvette cedex, France

²Département de Recherche en Electromagnétisme, LSS (UMR8506, CNRS-SUPELEC-Univ Paris Sud), 3 rue Joliot-Curie, 91192 Gif-sur-Yvette cedex, France

ABSTRACT. The design of an ultrasonic array and its settings for a specific inspection involves multiple parameters and is the result of a compromise between different requirements and limitations. Parametric studies based on simulation tools are often performed to ensure that the transducer has suitable performances in terms of detection of the defects sought. An automatic optimization tool, based on an evolutionary algorithm driving CIVA's simulation data, is proposed and tested in realistic applications to design inspection parameters (designing, positioning and/or setting the transducer).

Keywords: Ultrasonic, Optimization, Transducer, Phased-Array

PACS: 43.38.Hz, 43.35.Zc, 02.60.Pn

INTRODUCTION

The design of a phased-array transducer for ultrasonic non-destructive testing (UT) requires a guarantee of beam quality and minimization of the number of elements. The quality of the beam is given by its ability to respect prescribed depth, orientation and width which mostly depend upon aperture and frequency. Phased-array techniques can generate grating lobes which can be avoided by using the well-known value of inter-element pitch $d = \lambda / 2$ [1]. However, the number of elements is affecting the cost of the transducer and of its driving electronics. Then, the key is to ensure a good compromise between beam quality and cost.

Parametric studies are often automated via Evolutionary Algorithms (EAs) for dealing with such inverse problems [2]. For example, Lupien *et al.* [3] used an evolution strategy to design a transducer by looking for the emission surface shape which minimizes the number of rings of an annular phased-array; and Yang *et al.* [4] used a genetic algorithm to design a sparse array transducer.

The motivation of the present investigation is to propose an optimization tool to design probes for ultrasonic non-destructive testing, using the simulation platform CIVA [5] of CEA LIST as forward solution tool. The first section describes the optimization algorithm and an example of application on a nozzle inspection. In the second section, two

extensions which enable us to solve constrained and multi-objective problems are proposed. The third section presents an optimization problem of surrounded array design solved using the optimization tool. A brief conclusion ends this paper.

OPTIMIZATION ALGORITHM

Among many available EAs, which make non-trivial a choice, the Randomized Adaptive Differential Evolution (RADE) [6] has been chosen in view of its good performance in solving engineering optimization problems and its small number of tuning parameters. RADE aims at the evolution of a population of candidate solutions in order to build up an optimal solution. Next, the number of population members is written NP .

The i^{th} candidate solution at generation k is denoted as $X_i^{(k)}$ and is defined by the vector $X_i^{(k)} = [x_{i1}^{(k)}, \dots, x_{in}^{(k)}]$, wherein n is the number of variables of the problem. Its ability is measured by an objective function evaluated for this solution, noted $f(X_i^{(k)})$. In the present case, variables ($x_{ij}^{(k)}$) should correspond with CIVA parameters and objective functions are computed using forward ultrasonic models implemented within it [7-8]. Those obviously depend upon the problem at hand. As is usual, the candidate solution associated with the least value of the objective function is sought.

Randomized Adaptive Differential Evolution

RADE is derived from Differential Evolution [9], for which auto-regulation of the mutation factor is enforced. Standard evolutionary operators are used: mutation, crossover, and selection. The first step is the initialization of the population ($X_i^{(0)}$) by an uniformly distributed random set within the search range:

$$x_{ij}^{(0)} = x_j^L + rand \cdot (x_j^U - x_j^L) \text{ for } i = 1, \dots, NP \text{ and } j = 1, \dots, n \quad (1)$$

where $rand$ is a random real number between 0 and 1. At generation k , mutation creates new vectors ($V_i^{(k+1)} = [v_{i1}^{(k+1)}, \dots, v_{in}^{(k+1)}]$) by adding perturbations to a reference solution:

$$V_i^{(k+1)} = X_a^{(k)} + F_i \cdot (X_b^{(k)} - X_c^{(k)}) \quad (2)$$

where a , b and c are random integers between 1 and NP , F_i is the mutation factor, a self-adapted tuning parameter of the i^{th} candidate solution of the population [6], were $F_i \in [0.1, 0.9]$. Crossover yields vectors $U_i^{(k+1)} = [u_{i1}^{(k+1)}, \dots, u_{in}^{(k+1)}]$ by combining variables between the new and parent solutions:

$$u_{ij}^{(k+1)} = \begin{cases} x_{ij}^{(k)} & \text{if } rand > Cr \\ v_{ij}^{(k+1)} & \text{otherwise} \end{cases} \quad (3)$$

where $Cr \in [0.1, 0.7]$ is a user-defined parameter, called crossover rate. Last, the selection keeps solutions which improve on the objective function:

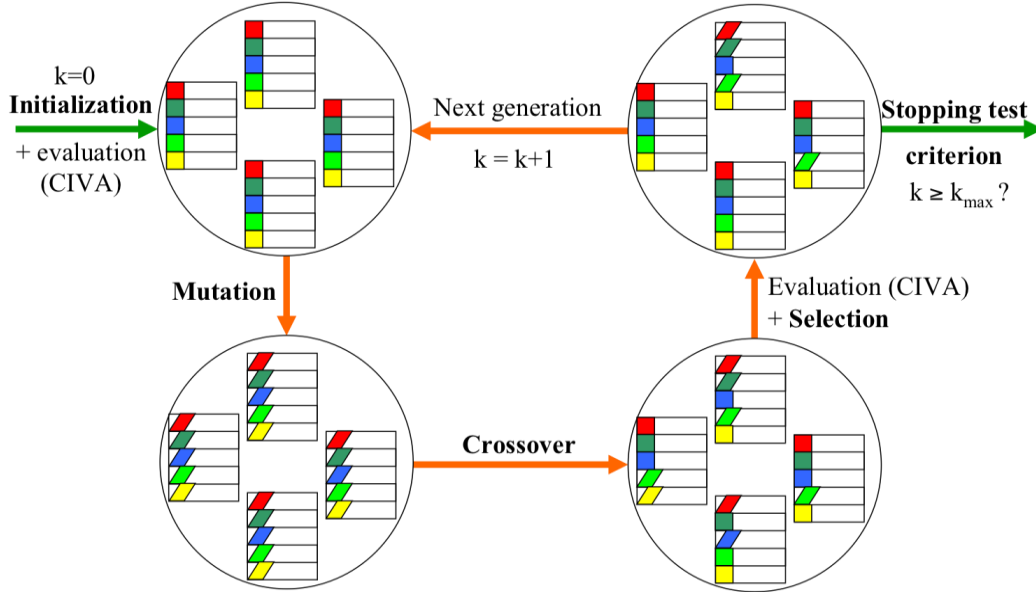


FIGURE 1. Differential Evolution diagram involving main evolutionary operators: initialization, mutation, crossover, and selection.

$$X_i^{(k+1)} = \begin{cases} U_i^{(k+1)} & \text{if } f(U_i^{(k+1)}) < f(X_i^{(k)}) \\ X_i^{(k)} & \text{otherwise} \end{cases} \quad (4)$$

This evolution, as illustrated in Fig. 1, is performed for the next generations ($k = k + 1$) until a stopping criterion is fulfilled. Here, the criterion is a maximum number of generation k_{\max} . Characteristic of the approach are three factors: population size (NP), a large value favoring robustness and a small value favoring speed (with the risk to only find a local optimum), crossover rate (Cr), a large value meaning intensive exploration of the search space and a small value intensive exploitation of history, and the number of generations (k_{\max}).

UT Application

This algorithm has been tested on a nozzle inspection, as illustrated in Fig. 2(a), to optimize the detection of one given planar flaw using a flexible 8×8 -element probe operated at 2 MHz frequency. The objective is to maximize the amplitude of the corner echo of a breaking back-wall flaw whose location is known. The variables of the problem are the position of the transducer: Y (vertical position), Θ (angular position) and α (rotation on itself); and of the focal point: r , θ and ϕ (in the spherical coordinate system). The main difficulty is to find the closest position of the probe to the defect, in order to focus in the near field and to reduce attenuation loss, for which the beam is as specular as possible on the defect.

The following values of tuning parameters have been used to perform this optimization: $Cr = 0.7$, $NP = 30$ and $k_{\max} = 100$, then 3030 candidate solutions have been generated. The computation time of 42 seconds for each simulation leads to about 36h total running time, on a standard PC. Beyond the 23rd generation, the optimization tool found a solution better, in terms of the objective function, than the one found by the expert (cf. Fig. 2(b)). The 33rd generation (convergence being achieved) associated to the final solution is 5 dB better (cf. Fig 3).

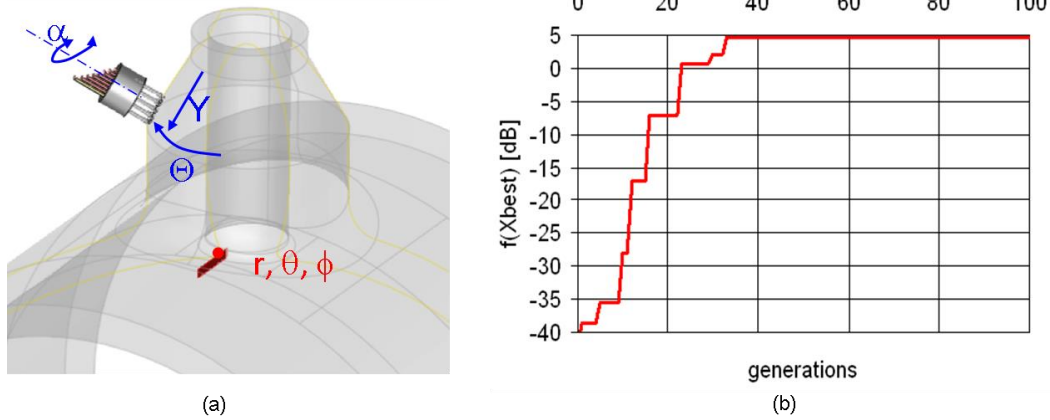


FIGURE 2. Optimization of a nozzle inspection. (a) Set-up of the inspection and definition of parameters involved for the optimization. (b) Evolution of the objective function of the best solution for each generation $k = 0, \dots, 100$. Values of the objective functions are given in dB compared to a solution found by an expert.

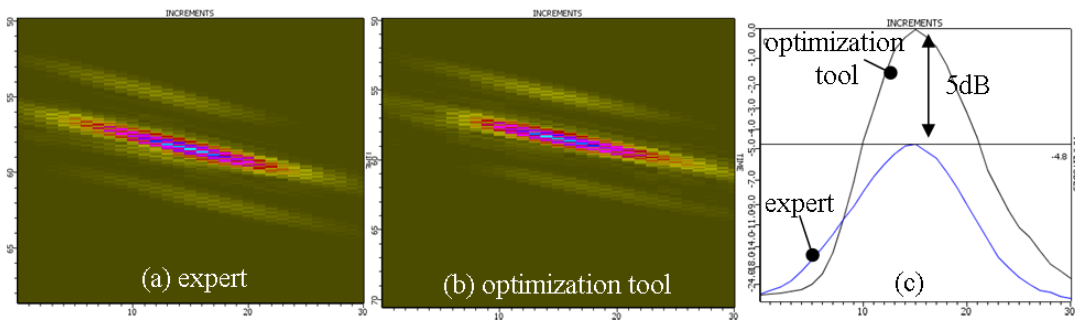


FIGURE 3. Imaging of the nozzle inspection. (a) B-Scan of the expert solution. (b) B-Scan of the optimization tool solution. (c) Comparison of echo-amplitude curve of solutions found by an expert and the optimization tool.

EXTENSIONS: CONSTRAINT & MULTI-OBJECTIVE

Some UT optimization problems have to take into account more *a priori* information to be efficiently solved. Then, RADE has been extended in order to solve constrained multi-objective problems.

Constraint Handling

Two kinds of constraints are considered: bounding-box and inequality constraints.

Bounding-box constraints are handled separately for each variable to guarantee that all solutions evaluated remain within search range. If a variable is outside, it is put back into it by symmetry on the closest boundary.

Inequality constraints are inequality relationships which involve several variables and have to be satisfied by the optimal solution. Then, according to Deb [10], a solution can be either feasible if it respects all constraints or unfeasible if it violates at least one. Consequently, feasible solutions are favored *vs.* unfeasible ones.

Multi-Objective Approach

An optimization problem is said to be multi-objective if more than one objective have to be optimized. Then, a vector-valued function is defined by $\mathcal{F}(X) = [f_1(X), \dots, f_{NO}(X)]$ where NO is the number of objectives. The main difficulty is

that two solutions cannot be easily compared, e.g., one objective might be better reached and another one less, or vice-versa. The so-called non-dominated sorting is often employed, as hereafter. The starting point is the dominance relation defined by [11]:

$$X_1 \text{ dominates } X_2 \Leftrightarrow \forall l \in [1, NO], f_l(X_1) \leq f_l(X_2) \text{ and } \mathcal{F}(X_1) \neq \mathcal{F}(X_2) \quad (5)$$

Obviously, solutions can be sorted out in order to produce non-dominated sets of solutions with an attached rank. Rank one, defined by S_1 , is the set of all solutions that are not dominated, and give all best compromises between all objectives and is our main target. Rank two, defined by S_2 , is the set of all solutions only dominated by some solutions from S_1 . And so on for the next ranks. This non-dominated sorting is illustrated in Fig. 4 for an example with two objectives.

Since candidate solutions can be ordered with non-dominated sorting, solutions from the same rank should be ordered to favor the most isolated ones, a good spread of solutions being aimed at within the Pareto optimal set. To achieve this goal, a diversity preservation method is applied, involving the crowding-distance [12]. Then the algorithm favors solutions from sets with lowest ranks that are the most isolated, so S_1 converges to the Pareto optimal set of the problem.

UT APPLICATION OF PHASED-ARRAY DESIGN

This section describes the application of these algorithms on a constraint multi-objective problem dealing with the design of a phased-array probe for UT. The inspection of a stainless steel pipe filled by water is sketched in Fig. 5. The probe, a surrounded array, has to detect axially oriented cracks with 45° compressional waves within the pipe wall. An electronic scan and a mechanical scan are respectively used for radial (in the plane (\vec{x}, \vec{y})) and axial (along the axis \vec{z}) inspections.

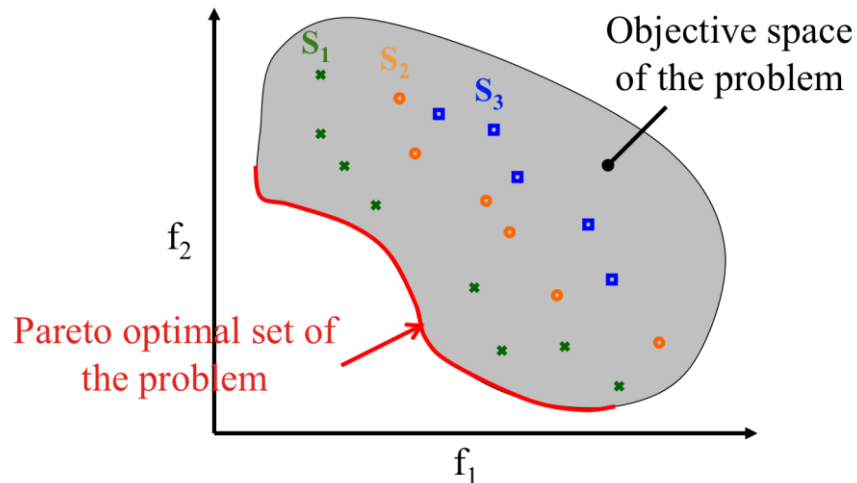


FIGURE 4. Illustration of the non-dominated sorting. Crosses, circles and squares are evaluated candidate solutions. Crosses define rank one, circles rank two, and squares rank three. The optimization aims at making S_1 to converge to the Pareto optimal set of the problem.

Les paramètres requis sont manquants ou erronés.

FIGURE 5. Inspection of a pipe using a surrounded array to detect axially oriented cracks.

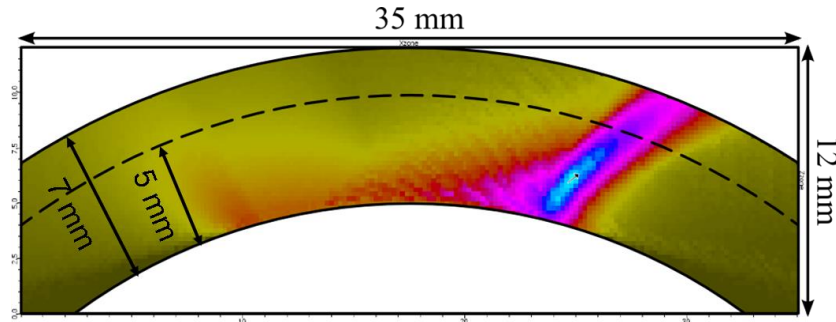


FIGURE 6. Field computation performed for an example of candidate solution that has a good grating-to-lobe ratio, but beam deviation and depth are not very satisfactory.

The probe design depends upon four variables: the orthogonal width, elements width (in the incident axis), gap between elements, and central frequency. Moreover, the electronic scanning sequence has to be set, and it depends upon three parameters: focusing depth and deviation angle of the delay law, and the number of elements used in the sequence. Then, candidate solutions are defined by six variables since the focusing depth is set on the outer surface of the pipe (5 mm in the component).

Objectives and Constraints

This application aims at finding the transducer's design and settings which produce the *best* beam. Quality is appraised by: the beam direction (45° on the defect) and depth (on the outer surface of the pipe), and the ratio of beam-to-grating-lobe amplitudes. The evaluation of these values is based on the transmitted field of compressional waves, computed with the pencil method [13]. Interactions on the outer surface of the pipe are not taken into account. As depicted in Fig. 6, the pipe is simulated with a larger depth than the real one in order to acquire more information about the beam in the outer surface's neighborhood.

To solve this problem, two objective functions (f_1 and f_2) are defined: f_1 aims at having a beam orientation as close as possible to 45° on the defect, and f_2 aims at maximizing the beam amplitude *vs.* the one of the grating lobe. Beam depth is taken into account in f_2 using a weighting coefficient. Moreover, one considers that the phased-array instrument limits the number of elements of the transducer to 256, and, that, due to manufacturing constraint, the element width cannot be smaller than 0.2 mm.

Results

The surrounded array design problem has been solved with the proposed optimization tool. The following values of tuning parameters have been used to perform this optimization: $Cr = 0.7$, $NP = 25$, $k_{\max} = 50$. So, 1530 candidate solutions have been generated among which 1422 were feasible. Since only feasible solutions are evaluated by running a CIVA field computation of about 2'10 long each on a standard PC, this leads to about a 50h total running time.

The Pareto optimal sets obtained every ten generations are depicted in Fig. 7. One can notice a convergence of the shape of Pareto sets since the 30th generation. At the 50th generation, the Pareto set is made of 94 solutions. Herein, one focuses on three candidate solutions (18, 21 and 22) and their displacement fields. They have been identified for their good ability to solve the problem with three kinds of compromises. Solution 18 has a better beam deviation than the two other solutions but some grating lobe effects and the focusing depth is in the middle range. Solution 21 well focuses on the outer surface but has

some grating lobes and a beam deviation in the middle range. Solution 22 has less grating lobes but does not focus as well as solution 21 on the outer surface and shows a beam deviation worse than the two other solutions.

One can point out that no solution leads to ideal compromise between all objectives, due to the constraints on the number of elements. This highlights the benefits of the Pareto set since it lets the end-user choose the best compromise in order to take into account other constraints not easily introduced in the optimization (e.g., manufacturing costs).

CONCLUSION

A hybrid differential evolution has been proposed to optimize probe designs and inspection procedures. It is able to handle constraints and to solve multi-objective problems so as to simplify end-user's utilization. Its efficiency in the design of a surrounded-array in order to generate the desired beam is shown. This test case in particular illustrates the interest of multi-objective optimization as yielding not only one solution but a set of solutions corresponding with different compromises. This optimization tool enables to deal with many different problems, e.g., positioning, setting and designing the transducer, here thanks to the use of CIVA ultrasound module as forward model. Yet the definition of objective functions appears as the main challenge to reach an appropriate optimum solution since it is not so easy to transform an engineering problem with all subtleties into a straightforward optimization one. In short, such a tool should be helpful to experts, not their substitute.

ACKNOWLEDGEMENTS

This work has been supported by the Région Ile-de-France within the framework of the CAPVERS project.

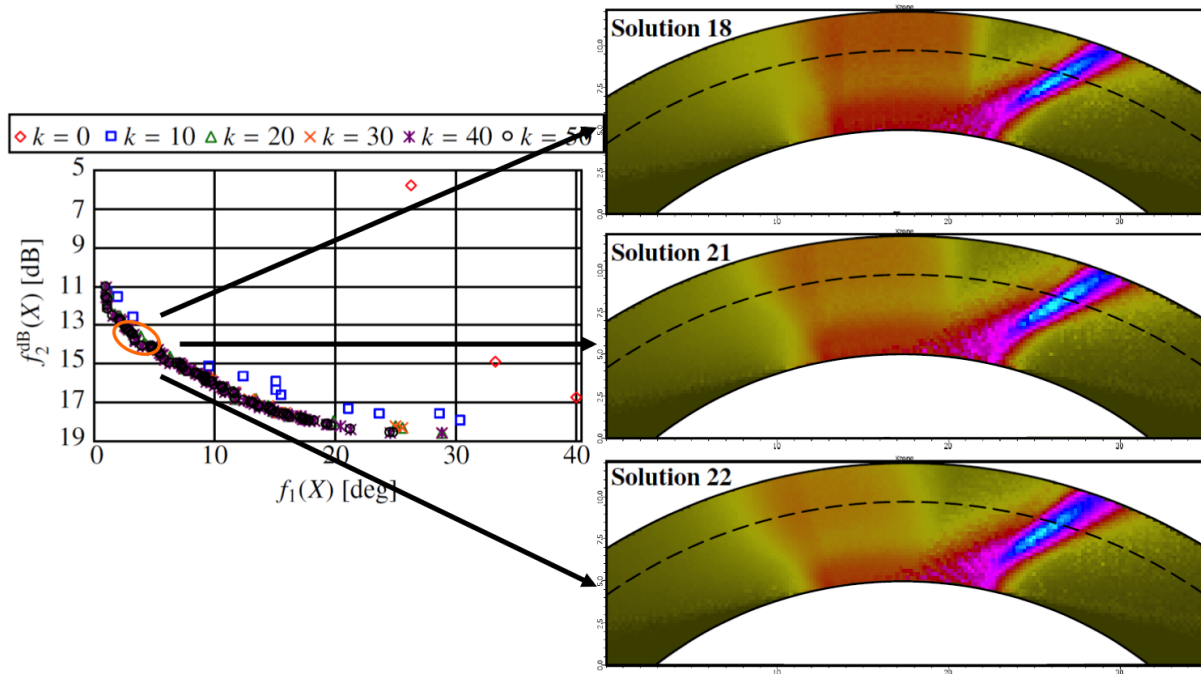


FIGURE 7. Pareto optimal sets obtained each 10 generations during the optimization of the surrounded array, and displacement field of solutions 18, 21 and 22.

REFERENCES

1. S. C. Wooh, Y. Shi, *Ultrasonics* **36**, pp. 737-749 (1998).
2. P. Rocca, M. Benedetti, M. Donelli, D. Franceschini, A. Massa, *Inverse Problems* **25**, 2009, 123003.
3. V. Lupien, W. Hassan, P. Dumas, "Improved titanium billet inspection sensitivity through optimized phased array design, part I: Design technique, modeling and simulation", in: *Review of Progress in QNDE*, D. O. Thompson and D. E. Chimenti, eds, AIP Conference Proceedings vol. 820, AIP, Portland, 2006, pp. 853-860.
4. P. Yang, B. Chen, K.-R. Shi, *Ultrasonics* **44**, e717-e721 (2006).
5. CIVA software platform for simulating NDT techniques (UT, EC, RT) <http://www-civa.cea.fr>
6. A. Nobakhti, H. Wang, *Applied Soft Computing* **8**, 2008, 350-370.
7. S. Mahaut, M. Darmon, S. Chatillon, F. Jenson, P. Calmon, *Insight – Non-Destructive Testing and Condition Monitoring* **51**, 2009, 78-81.
8. A. Lhémy, P. Calmon, I. Lecoeur-Taïbi, R. Raillon, L. Paradis, *NDT&E International* **33**, pp. 499-513 (2000).
9. K. V. Price, R. Storn, J. Lampinen, *Differential Evolution: A Practical Approach To Global Optimization*, Springer Berlin Heidelberg, New York, 2005.
10. Deb K, *Computer Methods in Applied Mechanics and Engineering* **186**, 2000, 311-338.
11. T. S. Angell, A. Kirsch, *Optimization Methods in Electromagnetic Radiation*, Springer-Verlag New York, 2004, pp. 239-284.
12. K. Deb, A. Pratap, S. Agarwal, T. Meyarivan, *IEEE Transactions on Evolutionary Computation* **6**, 2002, 182-197.
13. N. Gengembre, A. Lhémy, *Ultrasonics* **38**, 2000, 495-499.